POLITECNICO DI TORINO
Repository ISTITUZIONALE

Evaluation of Grid Harmonic Disturbances Injected by DC Electric Vehicle Charging Stations

Original
Evaluation of Grid Harmonic Disturbances Injected by DC Electric Vehicle Charging Stations / Benedetto, G., Bompard, E., Gugliotta, S., Mazza, A., Pons, E., Tosco, P., Zampolli, M., Jaboeuf, R.. - ELETTRONICO. - (2024), pp. 1-6. (2024 IEEE International Conference on Environment and Electrical Engineering and 2024 IEEE Industrial and Commercial Power Systems Europe (EEEIC / I&CPS Europe) Roma, Italy 17-20 June 2024) [10.1109/eeeic/icpseurope61470.2024.10751220].

Availability:
This version is available at: 11583/2994706 since: 2024-12-26T10:36:46Z

Publisher:
IEEE

Published
DOI:10.1109/eeeic/icpseurope61470.2024.10751220

Terms of use:

This article is made available under terms and conditions as specified in the corresponding bibliographic description in the repository

Publisher copyright
IEEE postprint/Author's Accepted Manuscript

©2024 IEEE. Personal use of this material is permitted. Permission from IEEE must be obtained for all other uses, in any current or future media, including reprinting/republishing this material for advertising or promotional purposes, creating new collecting works, for resale or lists, or reuse of any copyrighted component of this work in other works.

(Article begins on next page)

12 November 2026

Evaluation of Grid Harmonic Disturbances Injected by DC Electric Vehicle Charging Stations

Giorgio Benedetto
Dip. Energia & EC Lab
Politecnico di Torino
Torino, Italy
giorgio.benedetto@polito.it

Ettore Bompard
Dip. Energia & EC Lab
Politecnico di Torino
Torino, Italy
ettore.bompard@polito.it

Samuele Gugliotta
Dip. Energia & EC Lab
Politecnico di Torino
Torino, Italy
samuele.gugliotta@polito.it

Andrea Mazza
Dip. Energia & EC Lab
Politecnico di Torino
Torino, Italy
andrea.mazza@polito.it

Enrico Pons
Dip. Energia & EC Lab
Politecnico di Torino
Torino, Italy
enrico.pons@polito.it

Paolo Tosco
R&D and Techn. Innov. Dep.
Edison SpA
Milano, Italy
paolo.tosco@edison.it

Marco Zampolli
R&D and Techn. Innov. Dep.
Edison SpA
Milano, Italy
marco.zampolli@edison.it

Rémi Jaboeuf
R&D and Techn. Innov. Dep.
Edison SpA
Milano, Italy
remi.jaboeuf@edison.it

***Abstract*—The rapid adoption of Electric Vehicles requires advancements in Electric Vehicle Supply Equipment to accommodate the demand for enhanced performance. Commercial chargers now enable vehicles to inject power into the grid. However, the operation of the chargers introduces also distortions, in particular when multiple chargers operate simultaneously at the same node. This paper investigates the interaction between two different DC charging stations: one unidirectional and the other bidirectional. Then the analysis is extended to the harmonic interaction between the chargers. The results demonstrate the significant influence of the charger operation on grid power quality and highlight the importance of managing harmonic distortion.**

***Index Terms*—V2G, G2V, Stability, Filter, electric vehicle chargers, EV**

I. Introduction

The electrification of the transport sector requires the evolution of Electric Vehicle Supply Equipment (EVSE). As a result, modern charging systems support Vehicle to Grid (V2G) technology, allowing vehicles to function as generators. The operation of chargers affects grid power quality, as AC/DC conversion introduces current harmonic distortions. Electric Vehicles (EVs) can be charged using AC or DC, offering fast charges. Distortion issues worsen when multiple chargers operate simultaneously at a single network node.

In the work, the chargers have been supplied through amplifier for some reasons:

- Power amplifiers allow for precise control over the voltage and current supplied to the device under test.
- The power amplifiers can generate not only standard sinusoidal voltages, but also intentionally distorted voltages. This capability is crucial for testing how EVSEs respond to non ideal conditions, such as those caused by other equipment.
- Power amplifiers can adjust the load conditions dynamically during the tests. This allows for the evaluation of the performance under Variable Load Conditions.
- With a power amplifier, testers can perform more comprehensive evaluations, such as stress testing the EVSE under maximum power output and observing its behavior under abnormal conditions, which might not easily achieved using grid power.

Two different power amplifiers were tested to evaluate their impact on the harmonic distortion and power quality when connected to EVSE. The reason for testing two amplifiers, Linear Power Amplifier (LPA) and the Non Linear Power Pmplifier (NLPA), is to focus on their distinct capabilities regarding the supply of almost perfect sinusoidal versus distorted voltages and their respective influence on the power quality.

Furthermore, this work includes characterization tests of the unidirectional charger to evaluate the injected harmonic distortion, comparing these metrics against standard limits. Finally, the paper analyzes the harmonic interaction between the Unidirectional Charger (UC) and Bidirectional Chargers (BC) when connected to the same electrical node.

II. Literature Review

Power quality refers to how well the electricity delivered to electrical equipment matches the desired characteristics declared in standards. In Europe, the reference is the standard EN 50160 [1], that applies to public low, medium and high voltage AC electricity grids, under normal operating conditions. Any deviation in the voltage or current from the ideal value is a power quality disturbance. As expressed in the standard IEEE 1159-2019 [2], the main events that impact power quality are: voltage sag, voltage swell, voltage interruption, flicker, voltage and current distortion. The phenomenon considered in this work is the waveforms distortion, which is defined as a

This publication is part of the project NODES which has received funding from the MUR – M4C2 1.5 of PNRR with grant agreement no. ECS00000036 and of the project PNRR-NGEU which has received funding from the MUR - DM352/2022.

steady-state deviation from an ideal spectral content [2]. The analyzed distortion is the consequence of the operation of the EVSEs.

Due to the power electronic devices that are used in EVSEs, current harmonics are injected into the grid, and this leads to negative effects on transformers and cables, as described in [3] and [4].

It is important to highlight that the adverse effects are the more amplified the larger the aggregate of electric vehicles connected. This is verified in different researches as in [5], [6] and [7] which analyze the effect of an aggregation of multiple EVs connected to the same node of a grid. The results show that as the penetration level increases, the harmonic distortion of the grid also increases.

The standard IEEE 519-2014 [8] establishes the best practices for the design of electrical systems that include both linear and nonlinear loads, in order to limit the harmonic distortion impact on the grid. The limits are intended for application at a Point of Common Coupling (PCC) between the system operator and a user. The voltage limits are 5% for each harmonic order and 8% for the Total Harmonic Distortion $(\text{THD})_{\text{V}}\%$, as stated in the standard EN 50160 [1].

For each voltage range, the standard defines different sets of harmonic current limits, depending on the I_{SC}/I_L ratio, where I_{SC} is the maximum short-circuit current at PCC and I_L is the maximum demand load current (fundamental frequency component) at PCC, which would be the maximum current averaged over a demand interval (e.g. 15 minutes) for a given customer. As stated in [9], the ratio shows the relative impact that a given customer can have on the utility. In fact, a customer with a small demand relative to the short circuit current (I_{SC}/I_L large) may not cause much disruption to the utility system. Thus, such a customer is permitted higher harmonic current limits. Conversely, a large demand relative to the available fault current (I_{SC}/I_L small) faces stricter limits.

For each set of limits, the standard does not provide a limit on THD, but rather on Total Demand Distortion (TDD), which defines the global level of distortion as a percentage of the maximum demand load current I_L as calculated in equation (1).

$$TDD_I\% = 100 \times \frac{\sqrt{\sum_{h=2}^{h_{max}} I_h^2}}{I_L} \tag{1}$$

where:

- I_h is the rms values of the h-th current harmonic order;
- I_L is the maximum value of the load current;
- h_{max} is the last harmonic order considered in the analysis.

The difference between THD and TDD is that the first compares the momentary measured harmonics with the momentary measured fundamental current I_1, while the second compares the momentary measured harmonics with the maximum demand current I_L. However, in harmonic analysis, the index considered is the THD because, by definition, I_L will always be greater than I_1, therefore the TDD will always be less than the THD. In conclusion, if the THD meets the standard limits then the TDD will also meet the limits [9].

TABLE I
INDIVIDUAL CURRENT DISTORTION AND $\text{THD}_\text{I}\%$ LIMITS.

Odd harmonics		**Even harmonics**	
3^{rd} to 9^{th}	<4.0%	2^{nd} to 8^{th}	<1.0%
11^{th} to 15^{th}	<2.0%	10^{th} to 32^{nd}	<0.5%
17^{th} to 21^{st}	<1.5%		
23^{rd} to 33^{rd}	<0.6%		
35^{th} to 50^{th}	<0.3%		
$\text{THD}_\text{I}\%$		$\leq 5\%$	

From the previous considerations, the limits to which results obtained in the tests are compared are given in Table I [8].

III. LABORATORY SETUP

This paper presents laboratory tests conducted on real chargers. In this section, the laboratory equipment and setup used for these tests are described. Additionally, the laboratory connection scheme is showed in Figure 1.

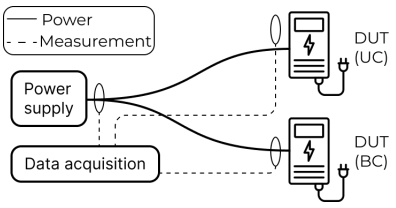


Fig. 1. Laboratory connection scheme

- **Linear power amplifier:** This technology has very high dynamic performance. It guarantees a simple interface and less instability issues. The power amplifier available is a Spherea Puissance Plus, which is a four quadrant 21 kVA (7 kVA per phase) linear amplifier that can be operated both in AC (three-phase) and DC, with four possible coupling modes. For the tests the Low Voltage Alternate Current (LVAC) 270 A was used.
- **Nonlinear power amplifier:** These amplifiers have lower accuracy and higher time delay compared to the linear ones, but they are less expensive and can be used for higher power applications, moreover this technology can be bidirectional without a derating during the V2G operations [10]. The DC chargers used for the experimental activities comes from different manufacturers. The first is a bidirectional wallbox of a rated power of 11 kW while the second is a new fast unidirectional charger of a nominal power of 47 kW.
- **Bidirectional charger:** The wallbox has a rated power of 11 kW when in Grid to Vehicle (G2V) state, while has a rated power of 10 kW when in V2G state.
- **Unidirectional charger:** This is a unidirectional fast charger with a rated and maximum charging power of 40 kW and 47 kW, respectively.

The vehicles available in the laboratory are two Nissan Leaf with a lithium-ion battery of 62 and 40 kWh, and with the CHAdeMO socket. However, in order to use the unidirectional charger it is needed to emulate a vehicle with the CCS Combo 2 socket through a dedicated device.

IV. METHODOLOGY

A. Measurements

The IEC 61000-4-7:2002 [11] is applicable to instrumentation intended for measuring spectral components in the frequency range up to 9 kHz which are superimposed on the fundamental of the power supply systems at 50 Hz and 60 Hz. According to the standard [11], the analogue signal which has to be analyzed is sampled, A/D-converted and stored. The Fast Fourier Transformation (FFT) is performed on a time window of *M* samples, and the window width T_N determines the frequency resolution $f_{res} = 1/T_N$, which is the frequency separation of the spectral components. Therefore, the window width T_N must be an integer multiple *N* of the fundamental period T_1 of the system voltage: $T_N = NT_1$. The sampling rate is $f_s = M/(NT_1)$, where *M* is the number of samples within T_N.

The standard specifies that for 50 Hz systems, the window width shall be of 10 fundamental periods ($T_1 = 20ms$), therefore the frequency resolution should be 5 Hz. Moreover, the last harmonic frequency to consider should be 2 kHz, which corresponds to the 40^{th} order.

The time window width and the frequency resolution are those suggested by the standard [11]. According to the Nyquist-Shannon sampling theorem, the minimum sampling rate should be 2 kS/s (related to the maximum frequency of 2 kHz), but in this case it is considered a sampling rate of 20 kS/s. From the sampling rate and the window width, the number of samples within the window is 4000.

B. Comparison of linear and nonlinear power amplifiers.

In order to test chargers of increasingly powers, these must necessarily be energized by the nonlinear amplifier, which allows to supply an higher power. Therefore, before implementing the switching amplifier in the tests, it is necessary to analyze whether the operating mode of the nonlinear amplifier influences the current harmonic distortion produced by the chargers. In fact, as described in [10], a nonlinear amplifier has lower losses than a linear amplifier. Nevertheless, if the output voltages have to be of very high quality, nonlinear amplifiers show significant limitations.

The objective of these tests is to compare the different behavior of the two power amplifiers, from a power quality point of view. The two amplifiers can supply the chargers with both purely sinusoidal and distorted voltages.

1) Testing procedure and selected parameters: For each of the two supply conditions, the same bidirectional wallbox has been powered by the LPA and by the NLPA , in both G2V and V2G configurations. The same vehicle, a Nissan Leaf of 62 kWh, has been connected to the charger.

In order to observe a gradual change in the harmonic content of the current, in all the test cases are considered $2\,\mathrm{kW}$, $5\,\mathrm{kW}$ and $10\,\mathrm{kW}$ as low, medium and high power set-points with respect to the charger's nominal value.

The electrical quantities are acquired and recorded and analyzed, computing the FFT. The currents are measured and analyzed for all phases, but since the system is balanced, the results of a single phase (L1) are discussed. The FFT provides the harmonic spectra from which the THDs% are computed and compared to the standard limits in Table I.

TABLE II
$THD_I\%$ WITH SINUSOIDAL AND DISTORTED SUPPLY VOLTAGES

Sinusoidal voltage supply				
Power [kW]	**NLPA [%]**		**LPA [%]**	
	G2V	**V2G**	**G2V**	**V2G**
2	6.40	6.61	6.09	5.97
5	3.29	3.34	3.13	3.19
10	2.22	2.06	2.24	2.10
Distorted voltage supply				
Power [kW]	**NLPA [%]**		**LPA [%]**	
	G2V	**V2G**	**G2V**	**V2G**
2	28.40	31.49	53.19	57.92
5	13.84	14.68	30.30	31.39
10	8.07	8.74	16.98	16.87

2) Sinusoidal supply voltage: With the same power set-point and operating state, the two amplifiers present very similar current harmonic spectra, except for some small differences with the currents supplied by the NLPA were slightly more distorted. The $THD_I\%$ is calculated up to the 40^{th} order, and is indicated in Table II, for the different power set-points, amplifiers and vheicle configurations.

The 5% limit on the $THD_I\%$ is exceeded only at a power set-point of $2\,\mathrm{kW}$, while already at $5\,\mathrm{kW}$ the limit is respected. This is due to the fact that $2\,\mathrm{kW}$ is a low power for the charger under test and the disturbances impact more on the THD measurement.

3) Distorted supply voltage: The supply voltage has been deliberately distorted with the following harmonic orders and their amplitudes set as percentages of the fundamental component (V_1), then the fifth harmonic $V_5 = 3\%V_1$, the fifteenth harmonic $V_{15} = 2\%V_1$ and the twenty-third harmonic $V_{23} = 2\%V_1$.

The harmonic orders selected are those most common in the Device Under Tests (DUTs) seen in previous works [5]. As expected, the currents are widely distorted. Comparing the individual harmonics at the same powers and operating configuration, it can be seen that the currents are much more distorted when provided by the LPA, and this is also evident for the $THD_I\%$ indicated in Table II. However, in standard conditions the two amplifier technologies demonstrated to be almost equivalent for our purposes, so, due to the higher output power the presented results are obtained feeding the chargers with the NLPA.

C. Harmonic interaction tests of UC and BC

The harmonic interaction of two identical DC chargers was analyzed in [5], where the DUTs was operating only in G2V mode. The results proved that the harmonic orders of current that can disturb the network tend to add up when operated at the same charging power. Therefore, by controlling the power set-points appropriately, the total harmonic distortion of grid current can be kept within the limits prescribed by the standard [8].

Differently, the tests described in this chapter aim to analyze the interaction of current harmonics due to the simultaneous

operation of the BCs and the UCs, which are of different manufacturer, power, and operating mode. Moreover, the interactions are analyzed in the following cases:

- UC in charging mode and the BC in discharging mode defined as G2V-V2G.
- both EVSEs in charging mode, defined as G2V-G2V.

The objective of the tests is to examine how the current harmonics individually injected by the chargers interact, amplifying or attenuating each other at the PCC.

The supply sinusoidal voltage is the nominal phase-to-neutral value of 230 V rms. For both G2V-G2V and G2V-V2G configurations, the five power set-point couplings of the chargers are indicated in Table III, and they are selected according to the following considerations:

- Both chargers with low power, with respect to their nominal values.
- Both chargers at the same power set-point, that is the rated value of the BC.
- The BC at its rated power and the UC at double of the set-point.
- The BC at a low set-point respect to its nominal value.
- Both chargers near their rated power values.

TABLE III
POWER SET-POINT CASES

Case	UC [kW]	BC [kW]
1	7	4
2	10	10
3	20	10
4	40	4
5	40	10

D. Testing procedure

For each case, tests are performed supplying the chargers from the NLPA. In each test case, are recorded the input of the UC, the input/output of the BC, and the output currents of the power source.

The limits recommended by the IEEE standard [8], shown in Table I, should be applied at the PCC, where the EVSEs interface with the grid. Therefore, the harmonic spectra and the $THD_I\%$ compared with the limits are those of the output current of the power source.

As described in [5], for quantifying the current harmonics interaction of the two chargers, defining how much the orders tend to add up in the power source current, the ratio between the total current to the source and the sum of the currents of the two DUTs is considered, for each harmonic order. The ratio is defined as the summation index k_s, computed with Eq. (2).

$$k_s = \frac{I_{PS}}{I_{UC} + I_{BC}} \tag{2}$$

where,

- I_{PS} is the current of the power source (NLPA or grid).
- I_{UC} is the input current of the UC.
- I_{BC} is the input/output current of the BC.

I_{PS}, I_{UC} and I_{BC} are array containing the harmonic content of the corresponding currents, up to 40th order, obtained by applying the FFT algorithm to the measured currents. Therefore, the summation index is defined for each harmonic order.

From its definition, the k_s is a number between 0 and 1, whose value expresses how much, for the same harmonic order, the currents of the two chargers add up.

Considering the cases in Table III, the EVSEs can work at very different powers, and this implies that in the summation index k_s, the contribution of the charger with lower power is negligible compared to the contribution of the charger with higher power, influencing the index more, which therefore tends to 1 more easily.

For this reason, to properly weight the contribution of the two chargers in k_s, the current of each device has been normalized with respect to its operating power dividing the analyzed current by the base current I_b, calculated with Equation 3.

$$I_{b,dev} = \frac{S_{dev}}{3 \times V_{rms}} \tag{3}$$

where:

- S_{dev} is the operating apparent power of the device in kVA;
- V_{rms} is the rms supply voltage (230 V rms) of the device.

In order to assess the magnitude of the current harmonics sum at the power source, in the Equation 2 the I_{PS} is normalized with respect to the sum of the base currents of the individual DUTs, while I_{UC} and I_{BC} are divided by their corresponding base currents.

Consequently, the normalized harmonic summation index assumes values between 0 (null sum) and $\frac{1}{2}$ (total sum). Therefore, in order to also define the normalized index in the range between 0 and 1, the ratio of Equation 2 is multiplied by 2 as in Eq. (4).

$$k_{s,norm} = 2 \times \frac{\frac{I_{PS}}{I_{b,UC}+I_{b,BC}}}{\frac{I_{UC}}{I_{b,UC}} + \frac{I_{BC}}{I_{b,BC}}} \tag{4}$$

The magnitude of $k_{s,\,norm}$ depends on two values:

- The amplitude of the harmonic with respect to the fundamental of the current considered, as normalization is done relative to the base current $I_{b,dev}$, whose amplitude is that of the fundamental component;
- The angular phase shift between the corresponding harmonics of I_{UC} and I_{BC} currents. The larger the phase shift the smaller the index value, and vice versa smaller phase shift implies tendency to add up more.

The phase shift is calculated with the Equation 5, from the complex currents of the chargers $\underline{I}_{UC}$ and $\underline{I}_{BC}$, obtained as the output of the FFT algorithm.

$$\Delta\phi = \angle\underline{I}_{\mathrm{UC}} - \angle\underline{I}_{\mathrm{BC}} \tag{5}$$

V. RESULTS

A. G2V-G2V

It can be observed that with all power couplings considered, each harmonic order complies with standard limits. Moreover, simultaneous operation of UC and BC does not produce excessive disturbances on the power source. This is confirmed by the $THD_I\%$ values in Table IV.

TABLE IV
THD$_I$% OF THE THREE CURRENTS FOR EACH POWER COUPLING

	7/4 kW	10/10 kW	20/10 kW	40/4 kW	40/10 kW
$\mathbf{I_{UC}}$	5,25	3,85	3,52	1,55	1,58
$\mathbf{I_{BC}}$	3,55	2,24	2,20	3,59	2,07
$\mathbf{I_{GE}}$	3,71	2,33	2,53	1,46	1,39

Similarly to [5], for each power coupling considered, the approximate values of the normalized summation index are calculated from Eq. (4), and their variations with the different tested operating powers of the DUTs are observed.

From Table V the 3rd harmonic always tends to sum, with a minimum value at the maximum power gap given in the 40/4 kW couple. Harmonics 5th and 7th seem to sum with varying percentages, regardless of the power couple, with minimum values reached when both chargers are working at the same power of 10 kW. Harmonics 11th, 13th and 23rd, tend to sum with lower percentages as the difference in powers increases, with minimum values reached at the 40/4 kW power couple. Therefore, it can be assumed that, for the power couplings considered, the operating condition in which globally a lower harmonic sum is obtained is the one with the largest gap between the operating powers of the chargers.

TABLE V
$k_{s,\ norm}$ FOR EACH HARMONIC ORDER AND POWER COUPLING IN G2V-G2V

Order	7/4 kW	10/10 kW	20/10 kW	40/4 kW	40/10 kW
3	1,15	0,90	1,11	0,76	1,16
5	0,79	0,56	0,74	1,02	0,83
7	0,99	0,16	0,33	0,51	0,90
11	0,56	0,57	0,89	0,21	0,79
13	0,89	0,98	1,06	0,21	0,29
23	1,23	0,81	0,63	0,25	0,35

The comparison between the 40/4 kW and 40/10 kW power couplings is graphically given in Figure 2. The first power couple is the best condition tested, while the second couple is given by the nominal powers of the two chargers. If a harmonic order tends toward the left in the Figures, it implies that those current harmonics of the chargers are less likely to sum. Conversely, the more a harmonic order is shifted to the right the more the harmonics are likely to sum. However, it is important to point out that the analysis need to be refined, since the results are obtained by considering only few measurements for each current, insufficient to define a probabilistic trend of a variable.

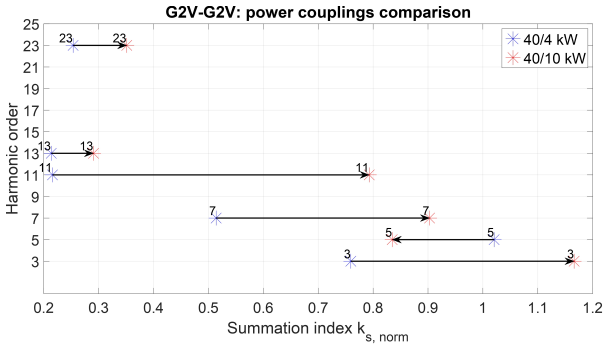


Fig. 2. $k_{s,\ norm}$ from 40/4 kW to 40/10 kW in G2V-G2V

B. G2V-V2G

In this operating configuration, the BC acts as a generator. Therefore, at the same power set-points, as with the 10/10 kW couple, the NLPA provides very low current implying higher harmonic amplitudes.

This is confirmed by the THD$_I$% values listed in Table VI, where it is evident that the total harmonic distortion of the I_{GE} current, averaged over the ten measurements, with the 10/10 kW couple is higher than the 5% limit, defined in [8]. In contrast, with the 40/4 kW couple, the current supplied by the NLPA is higher, therefore the harmonic distortion is greatly reduced.

TABLE VI
THD$_I$% OF THE THREE CURRENTS FOR EACH POWER COUPLING

	7/4 kW	10/10 kW	20/10 kW	40/4 kW	40/10 kW
$\mathbf{I_{UC}}$	5,14	3,73	3,66	1,64	1,60
$\mathbf{I_{BC}}$	3,51	2,07	2,30	3,73	2,09
$\mathbf{I_{GE}}$	9,26	21,03	6,90	1,84	2,07

By adopting the power couples in Table III, the analysis of the harmonic interaction has been performed, calculating the harmonic summation index, showed in Table VII, from the Eq. (4).

TABLE VII
$k_{s,\ norm}$ FOR EACH HARMONIC ORDER AND POWER COUPLING IN G2V-V2G

Order	7/4 kW	10/10 kW	20/10 kW	40/4 kW	40/10 kW
3	1,16	0,81	1,08	0,89	1,15
5	1,21	0,93	1,06	1,59	0,89
7	1,00	0,93	0,82	0,98	0,49
11	0,33	1,02	1,27	0,26	0,81
13	0,42	1,00	1,28	0,15	0,48
23	0,74	0,33	0,19	0,14	0,24

C. Probabilistic analysis

1) G2V-G2V: As described in [5], the power setpoints of the chargers are highly variable around the set values, therefore to define in a probabilistic way how the $k_{s,\ norm}$ is distributed during the operation of the DUTs, 100 current measurements have been recorded, to obtain the probability distributions of the $k_{s,\ norm}$, for each harmonic order. The tests are then performed in the power case 5.

Firstly, the Cumulative Distribution Function (CDF) is computed, in order to obtain the standard deviation and the mean value of the $k_{s,\ norm}$ for each harmonic order. The Table VIII shows the mean values of the $k_{s,\ norm}$ obtained from the distributions.

It can be seen that over 100 tests, averagely the 13th and 23rd tend to sum less than 50%, while the other harmonic orders tend to sum almost completely. On the other hand, the standard deviations for the 13th and 23rd are slightly higher than for the others, as also noted by the larger openness of their distribution. This implies that there are measurement cases in which the $k_{s,\ norm}$ is far from the mean value, although it never exceeds 60%.

2) G2V-V2G: As for the previous case, the Table VIII shows the mean values of the $k_{s,\ norm}$ obtained from the distributions. Also in this case it is obtained that over 100 tests, averagely the 3rd, 5th and 11th harmonics tend to sum

almost completely, while the 13th and 23rd orders tend to sum less than 50%. The only harmonic order that experiences a change in trend is 7th.

For the G2V-V2G case it must be considered that the reference angle is no longer 0°, as in the G2V-G2V configuration where the fundamentals of the current of the chargers are in phase, but 180° because the fundamentals are in opposite phase. Since the currents of the two chargers are in opposite phase, it can also be seen that in the G2V-V2G configuration, the I_{UC} lags behind the I_{BC}, for all harmonic orders considered and in most of the measurements executed.

TABLE VIII
$k_{s,\,norm}$ IN G2V-G2V AND 40 kW/10 kW

Order	Average $k_{s,\,norm}$ G2V-G2V	Average $k_{s,\,norm}$ G2V-V2G
3	1.15	1.15
5	0.83	0.87
7	0.91	0.5
11	0.78	1.03
13	0.4	0.31
23	0.31	0.22

D. Comparison between G2V-G2V and G2V-V2G

The $k_{s,\,norm}$ of both configurations, with the power case 5 are compared in Figure 3. It is emphasized how the 7th, 13th and 23rd harmonics tend to sum with lower percentages, while the 11th with higher percentage in the configuration G2V-V2G. For the 3rd and 5th harmonics, on the other hand, the indexes remain almost unchanged.

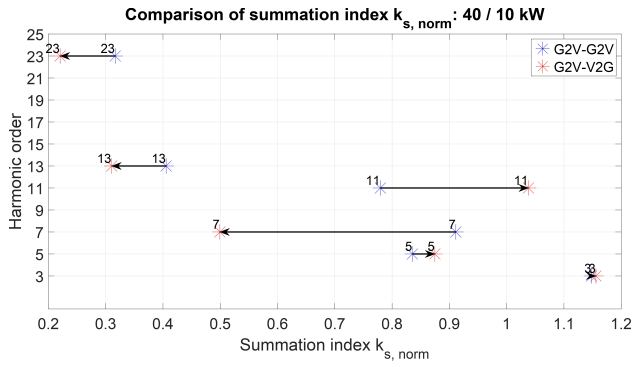


Fig. 3. Comparison of the $k_{s,\,norm}$ between G2V-G2V and G2V-V2G

VI. Conclusion

This research has provided a good example for understanding the effect of EV and EVSE on grid stability; the research focused also on the power amplifier technology showing that the diversity of the technology would not significantly affect the results of the research. In conclusion, the research has shown that determining and managing harmonic distortions from EV chargers is vital, especially when many devices are running and interacting at the same time.

From the k_s, norm values, averaged over the ten measurements, it was found that in G2V-G2V that the harmonics tended to add up with smaller percentages, whereas, in G2V-V2G this was confirmed only for the higher frequencies (11th, 13th and 23rd), while the lower ones tended to add up almost completely, regardless of the power couple. A more comprehensive probabilistic analysis was then performed with only the 40/10 kW rated power couple, acquiring 100 measurements of the three currents and 100 from which the PDFs of the ks, norm and were derived. From the PDFs of the ks, norm of both G2V-G2V and G2V-V2G configurations, it was found that on average the harmonic orders at high frequencies tend to add up with smaller magnitudes, compared with those corresponding to low frequencies, which tend to add up almost completely, as obtained from the approximate analysis. As expected, in the G2V-V2G configuration on average the harmonic contents tended to add up with less magnitude than in G2V-G2V, because currents were in the opposite phase. From the observed comparisons, in a system consisting of multiple chargers such as those analyzed, the harmonic distortion of the grid current might be most affected at the lowest harmonic orders that could greatly exceed the limits defined in the standards. However, when EVSEs are all charging, setting quite different powers can reduce the impact of harmonic interaction on the grid. Moreover, exploiting some units operating in V2G operation the harmonic cancellation could be improved. The future focus should be on improving the experimental uncertainty of harmonic interaction measurements and extending the probabilistic analysis to a wider range of tests for more extensive experimental coverage.

References

[1] *Voltage characteristics of electricity supplied by public electricity networks*, Std., 2022.

[2] "IEEE Std 1159-2019, IEEE Recommended Practice for Monitoring Electric Power Quality," 2019.

[3] M. Kazerooni and N. C. Kar, "Impact analysis of EV battery charging on the power system distribution transformers," in *2012 IEEE International Electric Vehicle Conference*. Greenville, SC, USA: IEEE, Mar. 2012, pp. 1–6.

[4] C. Zhou, H. Wang, W. Zhou, K. Qian, and S. Meng, "Determination of maximum level of EV penetration with consideration of EV charging load and harmonic currents," *IOP Conference Series: Earth and Environmental Science*, vol. 342, no. 1, p. 012010, Oct. 2019.

[5] A. Mazza, G. Benedetto, E. Bompard, C. Nobile, E. Pons, P. Tosco, M. Zampolli, and R. Jaboeuf, "Interaction among multiple electric vehicle chargers: Measurements on harmonics and power quality issues," *Energies*, vol. 16, no. 20, 2023.

[6] G. Benedetto, E. Bompard, A. Mazza, E. Pons, R. Jaboeuf, P. Tosco, and M. Zampolli, "Impact of bidirectional ev charging stations on a distribution network: a power hardware-in-the-loop implementation," *Sustainable Energy, Grids and Networks*, vol. 35, p. 101106, 2023.

[7] E. Alghsoon, A. Harb, and M. Hamdan, "Power quality and stability impacts of Vehicle to grid (V2G) connection," in *2017 8th International Renewable Energy Congress (IREC)*. Amman: IEEE, Mar. 2017, pp. 1–6.

[8] "IEEE Recommended Practice and Requirements for Harmonic Control in Electric Power Systems," IEEE, Tech. Rep., iEEE Std 519-2014.

[9] T. Blooming and D. Carnovale, "Application of IEEE STD 519-1992 Harmonic Limits," in *Conference Record of 2006 Annual Pulp and Paper Industry Technical Conference*. Appleton, WI, USA: IEEE, 2006, pp. 1–9.

[10] H. Ertl, J. Kolar, and F. Zach, "Basic considerations and topologies of switched-mode assisted linear power amplifiers," *IEEE Transactions on Industrial Electronics*, vol. 44, pp. 116–123, Feb. 1997.

[11] I. E. C. IEC, "Electromagnetic compatibility (EMC). Part 4-7, Testing and measurement techniques–general guide on harmonics and interharmonics measurements and instrumentation, for power supply systems and equipment connected thereto."